Renormalized molecular levels in a $Sc_3N@C_{80}$ molecular electronic device

Brian Larade,[1] Jeremy Taylor,[2,1] Q. R. Zheng,[3,1] Hatem Mehrez,[1] Pawel Pomorski,[1] and Hong Guo[1]

[1]*Center for the Physics of Materials and Department of Physics, McGill University, Montreal, PQ, Canada H3A 2T8*
[2]*Mikroelektronik Centret (MIC), Technical University of Denmark, East DK-2800 Kgs. Lyngby, Denmark*
[3]*Graduate School, The Chinese Academy of Sciences, Beijing, China*

We address several general questions about quantum transport through molecular systems by an *ab initio* analysis of a scandium-nitrogen doped C_{80} metallofullerene device. Charge transfer from the Sc_3N is found to drastically change the current-voltage characteristics: the current through the $Sc_3N@C_{80}$ device is double that through a bare C_{80} device. We provide strong evidence that transport in such molecular devices is mediated by molecular electronic states which have been renormalized by the device environment, such as the electrodes and external bias V_b. The renormalized molecular levels and main transmission features shift in energy corresponding to half the applied bias voltage. This is also consistent with our finding that the voltage drops by $V_b/2$ at each molecule/electrode contact.

The recent rapid progress of molecular electronics has opened up a new frontier whose aim is the ultimate miniaturization of electronic systems.[1–4] However, before moltronics becomes a viable technology, there remain many difficult challenges which must be solved. From a theoretical point of view, for example, a fundamental understanding of conduction at the molecular scale cannot be achieved by only considering the molecule and the electrodes *separately*. The entire system, molecule plus electrodes, must be investigated as a whole in a self-consistent manner including external bias potentials and charge transfer[5–7] which may occur when a functional molecule is bonded with electrodes: this molecule-environment interaction alters the original molecular levels that mediate transport. Of the many outstanding issues to be resolved, several stand out with particular significance in establishing a general physical picture for conduction through molecular junctions. If transport is mediated by molecular levels, what are these levels? How do these levels vary when the molecule is contacted by electrodes and put under an external bias voltage? Where is the bias voltage dropped? Which physical factors are critical in controlling current flow?

In this paper, we address these important issues and provide useful insights into molecular electronics by investigating the transport properties of endohedral metallofullerene molecular junctions. These molecular devices are themselves interesting from a moltronics and materials physics point of view, as it is very important to design device units by functionalizing electronically interesting molecules and to understand their electronic transport properties. More importantly, our first-principles investigation of these molecular junctions will shed light on a number of general features of transport at the molecular scale.

Our investigation is based on a recently developed self-consistent first-principles technique[6,8] which combines the Keldysh nonequilibrium Green's-function formalism[9–11] (NEGF) with a real-space self-consistent density-functional (DFT) method. The technical details of this NEGF-DFT method have been presented elsewhere[6,8] and we refer interested readers to them.

The system we investigate is in the form of $Al(100)$-$Sc_3N@C_{80}$-$Al(100)$ shown in the lower inset of Fig. 1(a), where the endohedral metallofullerene junction is formed by a C_{80} molecule encapsulating three Sc and one N atoms, and is bonded with atomic electrodes. The electrodes are modeled by $Al(100)$ atomic wires which extend to reservoirs at $\pm\infty$ where the current is collected. Recently, the metal containing endohedral fullerenes have attracted substantial interest[12] because these systems are expected to exhibit unusual material properties associated with charge transfer from the metal atoms to the carbon cage. Stevenson *et al.* reported a process which generates good fractions of milligram quantities of metallofullerenes[13] and they found that the Sc_3N cluster can be stabilized inside a highly symmetric, icosahedral C_{80} cage.

There are seven known C_{80} isomers,[14] and the experimental C_{80} endohedral metallofullerenes were found[13] to have I_h symmetry which is therefore the symmetry we choose. The Sc_3N cluster forms a planar triangle structure with N at the center of the triangle[13,15] [upper inset of Fig. 1(a)]. We use the x-ray experimental data[13] for the Sc_3N positions inside the C_{80} cage, with a Sc atom facing three pentagons within the cage. The Sc-N distance is fixed at 2.01 Å with N sitting at the center of the cage. An $Al(100)$ electrode is modeled by a semi-infinite Al atomic wire, consisting of Al slabs oriented along the (100) direction, with the closest Al-carbon distance fixed at 1.9 Å.

In Fig. 1(a), we show the I-V curves of the $Al(100)$-$Sc_3N@C_{80}$-$Al(100)$ molecular junction together with that of the $Al(100)$-C_{80}-$Al(100)$ system which has no Sc_3N. We have studied two orientations of the Sc_3N cluster: that with the Sc_3N plane parallel to the electrode surface (solid triangles); and that with the cluster plane along the transport direction (solid squares). Qualitatively, the two devices give similar I-V curves although the current is somewhat larger for the device when the Sc_3N plane is parallel to the electrode surface. Most notable, however, is the fact that devices with the Sc_3N cluster give a much larger current than those without, indicating that the endohedral metallo-
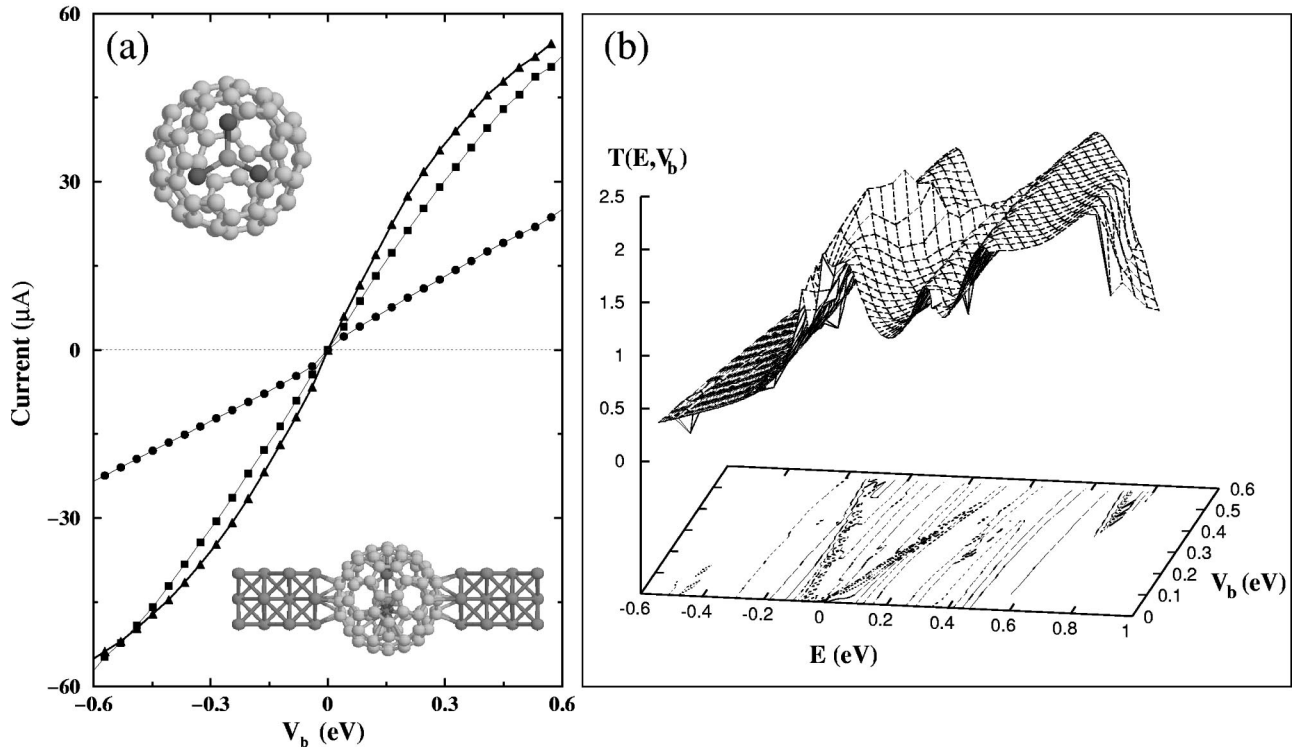
FIG. 1. (a) The I-V curves. Solid circles: for the Al(100)-C_{80}-Al(100) system. Solid triangles: for Al(100)-$Sc_3N@C_{80}$-Al(100) device with the Sc_3N complex plane parallel to electrode surface. Solid squares: for Al(100)-$Sc_3N@C_{80}$-Al(100) device with the Sc_3N complex plane perpendicular to electrode surface. Upper inset: the Sc_3N cluster situated inside the C_{80} cage, some C atoms have been removed in order to better view the Sc_3N. Lower inset: the molecular device with the electrodes extending to reservoirs at $\pm\infty$. (b) Total transmission coefficient $T(E,V_b)$ versus energy E and bias voltage V_b for the $Sc_3N@C_{80}$ device.

fullerenes are much better conductors than the corresponding bare C_{80} molecule. This increased conductance originates from the charge transfer from the Sc_3N complex to the C_{80}, thus aligning the molecular levels with the Fermi energy of the electrodes.

To understand the basic physics of transport through this molecular junction, we start by presenting an overall conductance picture by plotting the transmission coefficient $T(E,V_b)$ as a function of both incident electron energy E and bias voltage V_b. Figure 1(b) shows $T=T(E,V_b)$ for the $Sc_3N@C_{80}$ device with the Sc_3N plane oriented parallel to the electrode surface. Here it is important to notice that, while $T(E,V_b)$ is a complicated function of both external bias and energy, one may discern transmission features which shift when a bias potential V_b is applied. This shift is related to changes in electronic levels due to the influence of an external bias potential. This shift will depend both on how the levels couple to the electrodes and on the potential profile inside the molecule. Such information is not known *a priori* but it emerges naturally from our self-consistent *ab initio* analysis. Below, we will show that, by decomposing the total transmission in Fig. 1(b) into transmission eigenchannels,[16] one can obtain an understanding of the conduction through this device in terms of a set of molecular levels of C_{80} that have been renormalized by the environment (charge transfer and bias potentials).

In Figs. 2(a) and (b) we plot $T(E,V_b)$ as a function of a wider range of E for three values of V_b. For both devices,

transmission is dominated by features corresponding to the eigenstates of the C_{80} cage. An *isolated* C_{80} with I_h symmetry has a fourfold degenerate highest occupied molecular orbital (HOMO) containing two electrons, and a fourfold degenerate LUMO. When the C_{80} molecule is contacted by two Al(100) electrodes, our calculation indicates that there are approximately 4.7 charges transferred from the electrodes to the C_{80} cage. This charge transfer fills the HOMO level to $\sim84\%$ and the LUMO remains empty. For the $Sc_3N@C_{80}$ device, whose transmission coefficient is shown in Fig. 2(a), our investigation finds that the C_{80} again accepts ~4.7 charges from the electrodes. Furthermore, each Sc atom loses ~1.7 charges while the N acquires ~0.9, resulting in a net transfer of ~8.9 charges from the electrodes and the Sc_3N complex to the carbon cage. Together with the two electrons originally occupying the C_{80} HOMO,[17] they would completely fill the HOMO and partially fill the degenerate LUMO to $\sim36\%$. The Al(100)-$Sc_3N@C_{80}$-Al(100) device is therefore expected to be a better conductor than the Al(100)-C_{80}-Al(100) device at equilibrium, because the conduction is through a band which is closer to half filling.

The above discussion is based on a simple argument of filling levels of an *isolated* molecule. A quantitative analysis should consider the fact that the molecule is contacted by electrodes and the device is under a bias voltage such that the levels of the *isolated* molecule are affected. For an isolated molecule, one obtains the molecular levels by diagonalizing
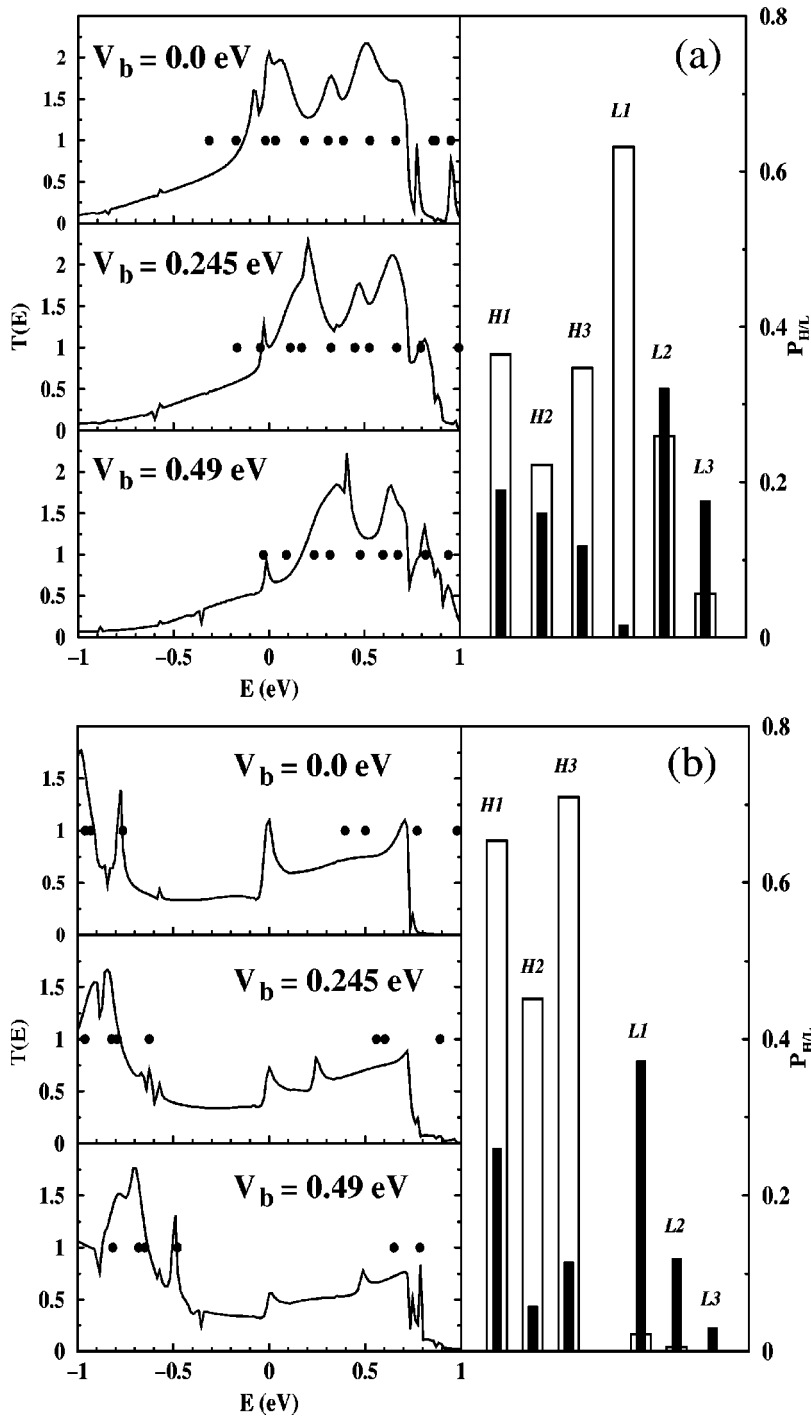
FIG. 2. Panels on the left: total transmission coefficient $T(E, V_b)$ versus E for three values of bias voltage. (a) For the Sc$_3$N@C$_{80}$ device; (b) for the bare C$_{80}$ device. Solid circles: the positions of renormalized molecular levels. Panels on the right: the projection coefficients $P_{H,L}$ of six RML's, projected onto the HOMO (white columns) and LUMO (black columns) of the original isolated molecule. H1–3 indicate the three closest RML's below E_F, L1–3 above E_F.

the Hamiltonian matrix $H_{\mu\nu}$ constructed from the atomic orbitals that describe the valence shell electrons in the molecule. This is impossible to do for our molecular device because the energy spectrum is continuous and the molecular levels acquire a finite width due to the coupling to the electrodes. To obtain a physical picture of the molecular electronic properties when the molecule is interacting with its environment, we found the following procedure quite useful. After the self-consistent iteration of the Kohn-Sham equation is completed,[6,8] we obtain the self-consistent Kohn-Sham effective potential $V_{\text{eff}}(\mathbf{r}, V_b)$ and Hamiltonian matrix $H_{\mu\nu}$. We then diagonalize the submatrix of the Hamiltonian asso-

ciated with the atomic orbitals in the molecule. The levels obtained in this way are therefore derived from the molecule interacting with the electrodes under bias, and we will refer to them as "renormalized molecular levels" (RML's). Since $H_{\mu\nu}$ was obtained in the presence of the electrodes and bias potential, this procedure gives a very good correspondence between the transmission peaks and the RML's. The RML positions are shown in Figs. 2(a) and (b) as solid circles. It is clear that there is an abundance of RML's where the transmission coefficient is large, suggesting that the transport is mediated by RML's. For the Sc$_3$N@C$_{80}$ device there are a number of RML's near the Fermi level, in contrast to the bare
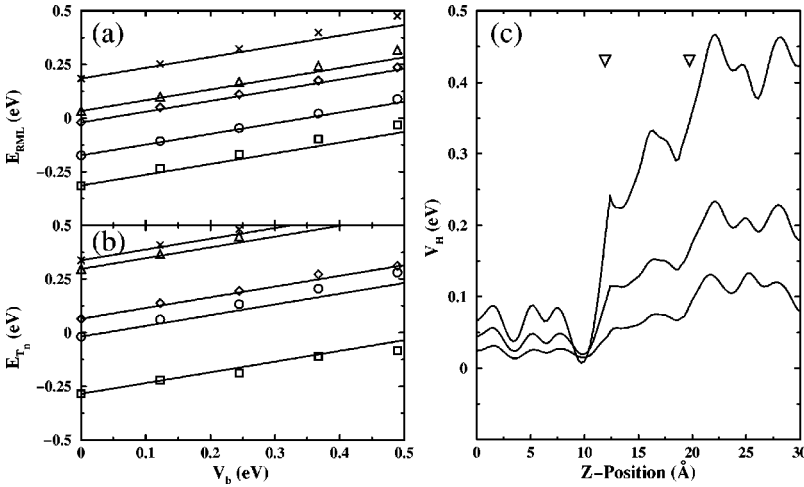
FIG. 3. (a) Five renormalized molecular levels, and (b) several peak positions of transmission eigenvalues near E_f versus bias voltage V_b for the $Sc_3N@C_{80}$ device. Solid lines indicate a fit with slope 1/2. (c) The Hartree potential V_H across the $Sc_3N@C_{80}$ device for three values of V_b, as a function of coordinate z for fixed x,y coordinates. From the bottom, $V_b = 0.12$, 0.245, 0.49 eV. The two inverse triangles indicate the starting and ending z coordinates of the carbon cage.

C_{80} device, indicating the Sc_3N doped C_{80} should have larger current, which is what we have found. We note that, because of the finite width of the renormalized molecular levels, there is still a substantial conductance at the Fermi level for the bare C_{80} device,[18] $G \approx 0.5 G_o$.

Our analysis suggests that the RML's can be related to the molecular levels of the isolated molecule. For example, for the bare C_{80} device, we can clearly see the RML's below and above E_f, which correspond to the fourfold degenerate HOMO and LUMO of the isolated molecule. Since the HOMO is filled, the Fermi energy lies in the gap between the HOMO and LUMO as expected. The character of the RML states $|\varphi^{RML}\rangle$ can be examined by projecting them onto the original HOMO states $|\phi^H\rangle$ and LUMO states $|\phi^L\rangle$ of the isolated molecule, in a spirit similar to the fragmented orbital analysis.[19] The right-hand panels of Figs. 2(a) and (b) show the projection coefficient $P_{H,L} \equiv |\langle \varphi^{RML} | \phi^{H,L} \rangle|^2$ for the six (labeled H1–3, L1–3) RML's nearest to E_f, projected onto the isolated molecular HOMO states (white columns) and LUMO states (black columns). Thus, for example, RML H1 of Fig. 2(b) has $\sim 65\%$ "HOMO character" and $\sim 25\%$ "LUMO character"; while RML L2 of Fig. 2(a) has $\sim 27\%$ "HOMO character" and $\sim 33\%$ "LUMO character." When we project these RML's nearest to E_f onto isolated molecular states away from the HOMO/LUMO, the projection coefficients are smaller by at least one order of magnitude, indicating that the RML's responsible for transport have indeed originated from the HOMO/LUMO states of the isolated molecule. This is why the above discussion, based solely on filling levels of the *isolated* molecule, gives a qualitatively sensible explanation that the $Sc_3N@C_{80}$ devices should have a larger conductance.

The role of the RML's can be further elucidated by studying their evolution as a function of bias voltage V_b. Our data shows that the RML's shift as a bias is applied: $E_{RML} \approx E_{RML} + V_b/2$. This is shown in Fig. 3(a) where the eigenenergies E_{RML} of five RML's near E_f are plotted versus V_b for the $Sc_3N@C_{80}$ device. The RML's also play a dominant role in transmission through the molecule under a bias voltage. The transmission coefficients in Fig. 2 have broad peaks and valleys differing by about one unit. The peaks, at both zero or finite bias, occur at energies where there are

RML's. Because the RML's shift by $V_b/2$, the transmission coefficients also shift by approximately $V_b/2$ in addition to changing shape. To see this clearly, we decompose the total transmission in Fig. 2 into transmission eigenchannels $T_n(E)$ by diagonalizing the scattering matrix.[16] Each eigenchannel $T_n(E)$ has an energy E_{T_n} where $T_n(E)$ is maximized. In Fig. 3(b), we have plotted the peak position E_{T_n} versus bias potential V_b for several eigenvalues near E_f. Clearly, the position of the peaks follows the bias potential and positions of the RML's: $E_{T_n} \approx E_{T_n} + V_b/2$. Exactly the same behavior is obtained for the bare C_{80} device.[18] These results suggest that the external bias voltage should drop by $V_b/2$ at each molecule-electrode contact. This is confirmed by investigating the Hartree potential V_H, shown in Fig. 3(c) for a slice of $V_H(x,y,z)$ along the transport direction for three biases. Although the overall behavior is very complicated due to the atomic cores, we observe that $V_H(z)$ indeed drops predominately at the contacts.

In conclusion, our results clearly suggest that conduction in the molecular devices studied here is mediated by *renormalized molecular levels*. In a molecular electronic device, the bare molecular levels are modified, or renormalized, by environmental factors such as charge transfer and bias, in ways that are difficult to predict *a priori*. However, our self-consistent analysis yields the self-consistent Hamiltonian matrix and corresponding RML's. These RML's have been shown to be a useful means to understand transport in such molecular devices. For example, in addition to charge-transfer doping from the electrodes, the presence of the Sc_3N metal complex and its associated charge transfer to the C_{80} cage aligns the RML's with the electrodes' Fermi level, thus doubling the current as compared with a bare C_{80} device. More interestingly, we found that those RML's responsible for conduction originate largely from the HOMO and LUMO of the original isolated molecule and that, under a bias potential, the transmission peaks and the renormalized molecular levels shift by $V_b/2$. This is a consequence of the fact that the electrostatic potential drops by $V_b/2$ at each metal-molecule junction. This potential profile is not universal. Indeed, a recent study of a benzene-1,4-dithiol molecule con-

nected to Au chains[20] has found that the voltage drops predominately at one contact. However, studying the RML's of a given molecular device and their evolution under a bias potential may well lead to clues in understanding the shape of the potential profile and its relationship to the original isolated molecular levels.

[1] C.P. Collier, G. Mattersteig, E.W. Wong, Y. Luo, K. Beverly, J. Sampaio, F.M. Raymo, J.F. Stoddart, and J.R. Heath, Science **289**, 1172 (2000).

[2] M.A. Reed, C. Zhou, and C.J. Muller, Science **278**, 252 (1997); J. Chen, M.A. Reed, and A.M. Rawlett, *ibid.* **286**, 1550 (1999).

[3] C. Joachim, J.K. Gimzewski, R.R. Schlitter, and C. Chavy, Phys. Rev. Lett. **74**, 2102 (1995); J.K. Gimzewski and C. Joachim, Science **283**, 1683 (1999).

[4] T. Rueckes, K. Kim, E. Joselevich, G.Y. Tseng, C.-L. Cheung, and C.M. Lieber, Science **289**, 94 (2000).

[5] N.D. Lang and Ph. Avouris, Phys. Rev. Lett. **84**, 358 (2000).

[6] J. Taylor, H. Guo, and J. Wang, Phys. Rev. B **63**, 121104 (2001).

[7] J. J. Palacios, A. J. Pérez-Jiménez, E. Louis, and J.A. Vergés, Phys. Rev. B **64**, 115411 (2001).

[8] The technical details are reported elsewhere, J. Taylor, H. Guo, and J. Wang, Phys. Rev. B **63**, 245407 (2001).

[9] A.P. Jauho, N.S. Wingreen, and Y. Meir, Phys. Rev. B **50**, 5528 (1994).

[10] S. Datta, *Electronic Transport in Mesoscopic Systems* (Cambridge University Press, New York, 1995).

[11] B.G. Wang, J. Wang, and Hong Guo, Phys. Rev. Lett. **82**, 398 (1999); J. Appl. Phys. **86**, 5094 (1999).

[12] For a recent review, see, for example, A.V. Eletskii, Phys. Usp. **43**, 111 (2000)[Uspekhi Fizicheskikh Nauk, **170**(2), 113 (2000)], and references therein.

[13] S. Stevenson, G. Rice, T. Glass, K. Harich, F. Cromer, M.R. Jordan, J. Craft, E. Hadju, R. Bible, M.M. Olmstead, K. Maitra, A.J. Fisher, A.L. Balch, and H.C. Dorn, Nature (London) **401**, 55 (1999).

[14] K. Nakao, N. Kurita, and M. Fujita, Phys. Rev. B **49**, 11415 (1994).

[15] M. Takata, E. Nishibori, M. Sakata, M. Inakuma, E. Yamamoto, and H. Shinohara, Phys. Rev. Lett. **83**, 2214 (1999).

[16] The sum of all transmission eigenvalues obtained from the scattering matrix gives the total transmission coefficient shown in Fig. 2. For discussions of this concept, see M. Brandbyge, M.R. Sorenson, and K.W. Jacobsen, Phys. Rev. B **56**, 14956 (1997).

[17] In order to use this comparison between the HOMO and LUMO states of the $Sc_3N@C_{80}$ device and the bare C_{80}, we must determine the character of these states. Our analysis finds the character of the HOMO and LUMO eigenstates for the $Sc_3N@C_{80}$ device to be ''carbonlike,'' with contributions from Sc and N less than 15%.

[18] There is one exception to the pattern of peak shifting by half the bias: the peak at $E=0$ in Fig. 2(b) actually splits into two when there is a bias, with one fixed at $E=0$ while the other shifts by the full V_b. Our investigation confirmed that this peculiar behavior was related to coupling of electronic bands in the electrode to that of the bare C_{80} molecule. Essentially, it is due to the relative shift in energy scale of the two electrodes which is given by eV_b.

[19] For a review, see, for example, R. Hoffmann, Rev. Mod. Phys. **60**, 601 (1988).

[20] M. Brandbyge, K. Stokbro, J. Taylor, J.-L. Mozos, and P. Ordejón, in *Nonlithographic and Lithographic Methods of Nanofabrication–From Ultralarge-Scale Integration to Molecular Electronics*, edited by L. Merhari, J. A. Rogers, A. Karim, D. J. Norris, and Y. Xia, Mater. Res. Soc. Symp. Proc. **636** (Materials Research Society, Pittsburgh, 2001).